100 GbE Passive Optical Access Networks Technical Milestone Report

Adrian I. Lam
Supervised by Dr. Seb Savory
16 January 2019

Abstract

This project aims at evaluating methods of achieving a 100 Gb/s Ethernet passive optical access network. An optical link based on coherent receivers will be considered, and a computer model will be built using MATLAB® to simulate various physical effects in the optical fibre. Digital signal processing techniques will be employed to correct for these effects and demodulate the transmitted symbols. Currently, all relevant linear effects have been successfully simulated and compensated for, while non-linear effects have not been completed yet. After the model is complete, different designs of the network, such as using different modulation schemes or multiplexing methods, can be simulated and their performance compared, and the feasibility to use them in an access network will be discussed. The results may also be verified through off-line processing of real measured data.

1 Introduction and Motivation

A passive optical network (PON) is a point-to-multipoint system where data for all users of the network, modulated onto an optical signal, leaves the optical line terminal at the service provider, and is carried along a fibre feeder, then split by an unpowered beam splitter, without any routing or selection, to separate distribution fibres reaching the optical network units of the users [1, §6.1]. This design allows high-speed communication for a large number of consumers, with relatively low cost for each user [2], and is currently typically employed in a fibre-to-the-home setting [3].

Fibre-to-the-home applications are already well-served by the currently mature implementation of 1 Gb/s PONs, which may make higher speed PON seem unnecessary. However, there are many more future applications that could potentially benefit from a 100 Gb/s PON. By designing future PON specifications to be compatible with existing fibre installations, less installation costs will be incurred, allowing the mixing of more applications onto the same network, thus increasing revenues for service providers. In addition, as more and more people rely on mobile networks for their daily communication and entertainment needs, mobile operators are looking to increase the density in cell sites, making PONs a good candidate to deliver the cell data backhaul. As the 5G mobile standard develops, PONs may even be useful in the fronthaul, where radio signals were sampled and relayed, through a PON, to a centralized location for digital signal processing (DSP), seen as a way to reduce costs [3].

The use of coherent receivers in a high-speed PON is considered. In contrast to direct detection receivers, both the real and imaginary parts of each polarization of the received electrical field can be detected separately in a coherent receiver. This makes complex modulation schemes such as phase-shift keying (PSK) or quadrature amplitude modulation (QAM) possible, and combined with polarization-division multiplexing (PDM), makes very high data rates possible [4, §5.6], [5].

In this project, a model to simulate the various physical effects in an optical channel is to be built. DSP will then be used to attempt to correct for these effects to recover

the original signal. Using this model, different options for achieving a 100 Gb/s PON will be compared. The response of a real channel will then be measured and, using the DSP techniques investigated, processed offline to verify the model and the correction methods. Feasibility of employing these techniques in a commercial PON setting will also be discussed.

The current progress in developing the simulation model is detailed in Section 2, with future plans listed in Section 3.

2 The Simulation Model

Figure 1 shows the current basic model, involving a transmitter with a root-raised cosine pulse shaping filter, processed to simulate the various physical effects, then transmitted through an additive white Gaussian noise (AWGN) channel to a receiver with a matched filter. The received signal is then sampled and DSP is used to correct for the physical effects in the electrical domain. The demodulated signal is then compared to the original pseudorandom data, to obtain a measurement of the bit-error rate (BER) using a Monte-Carlo approach. Currently, the main modulation scheme considered is quadrature phase-shift keying (QPSK), with Gray coding.

The effects considered are enumerated below. The results of the methods used to correct for the effects are compared to the ideal AWGN channel.

2.1 Chromatic Dispersion

Chromatic dispersion (CD) is the effect of the group speed of light varying with the wavelength of the optical signal [4, §2.7.3]. It can be modelled as a linear system, with transfer function in the Fourier domain

$$G(z,\omega) = \exp\left(-\mathrm{j}\frac{D\lambda^2 z}{4\pi c}\omega^2\right)$$

or with impulse response in the time domain

$$g(z,t) = \sqrt{\frac{c}{\mathrm{j}D\lambda^2 z}}\exp\left(\mathrm{j}\frac{\pi c}{D\lambda^2 z}t^2\right) \quad (1)$$

with z being the transmitted distance, c the speed of light in vacuum, λ the wavelength in vacuum, and D the dispersion parameter of the fibre [5]. For all simulations below, $D = 17\,\mathrm{ps/(nm\,km)}$.

Using this model, constellation diagrams were obtained and shown in Figure 2. It can be seen that over long distances, CD would make demodulation very difficult, and as such, it is necessary to compensate for this effect. Current systems use dispersion compensating fibres, but DSP may be applied instead to reduce cost [5]. It is noted that by inverting the sign of D in Equation (1), the impulse response of the dispersion compensating filter is obtained, and with truncation and discretization, can be implemented as a simple tapped delay line [5].

Figure 3 shows the dispersion compensating filter in action. The resulting BER very closely resembles that of the ideal AWGN, thus verifying the implementation.

2.2 Adaptive Equalizer

Adaptive equalizers can be used to correct for time-varying effects, an example of which is polarization dependent effects. [5] discusses the implementation of adaptive equalization to PDM signals. This has yet to be implemented in the simulation model.

On the other hand, an implementation for a single polarization state has been done. This would be useful for correcting for fluctuations to the environment [4, §11.6.1], not simulated in the model, but would be present in real life. In addition, it was observed that the CD compensating filter discussed in Section 2.1 does not perform very well over short distances, as can be seen in Figure 4, due to truncation of the non-causal infinite-length impulse response. Adaptive

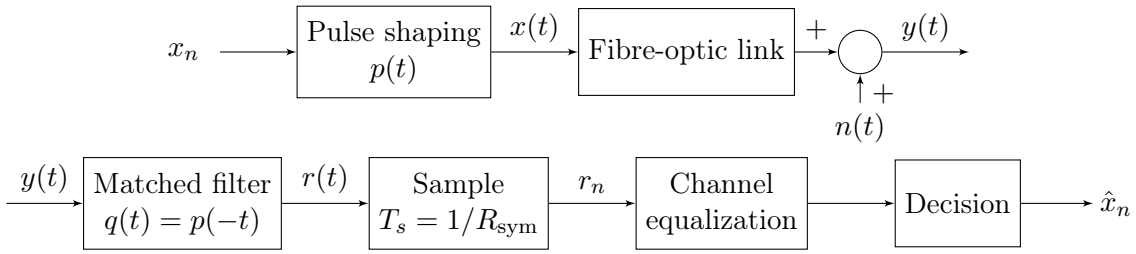

Figure 1: Block diagram of the simulation model.

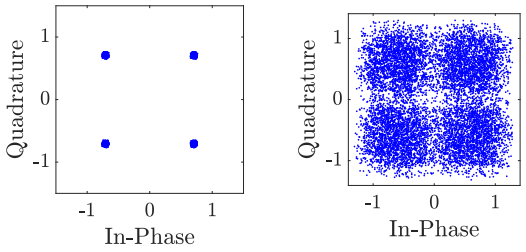

(a) $z = 1\,\text{km}$. (b) $z = 5\,\text{km}$.

Figure 2: QPSK constellation after chromatic dispersion, without AWGN.

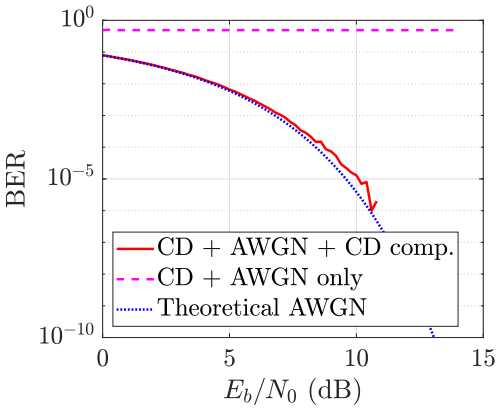

Figure 3: QPSK signal with simulated chromatic dispersion and CD compensation, over an AWGN channel, with $z = 200\,\text{km}$.

equalization was attempted to correct for this effect as well.

Two types of equalizing algorithms are typically considered, namely the constant modulus algorithm (CMA) and the decision-directed least mean square (DD-LMS) algorithm [4, §11.6.1]. CMA has been implemented due to its simplicity. If time permits, DD-LMS can also be attempted.

The CMA relies on the fact that for PSK signals, the transmitted symbols all have unit amplitude. As a result, it attempts to minimize the distance between the signal and the unit circle. Figure 5 illustrates the adaptive nature of the algorithm. Figure 4 demonstrates the success of the CMA, bringing the performance curve back to the theoretical values.

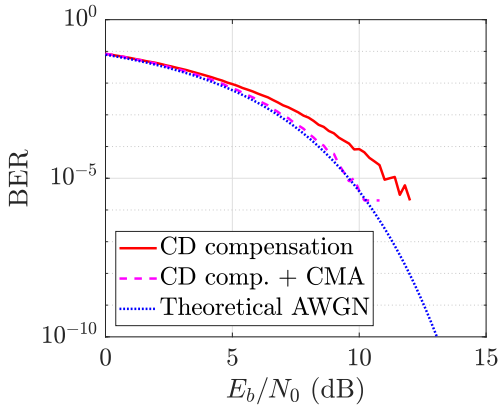

Figure 4: QPSK signal with CD, CD compensation, and CMA adaptive equalizer, over an AWGN channel, with $z = 2\,\text{km}$.

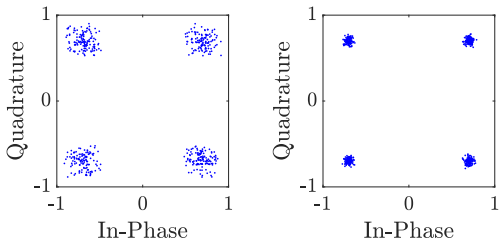

(a) Symbols 1 to 500. (b) Symbols 2001 to 2500.

Figure 5: Constellations showing the adaptive behaviour of the CMA.

2.3 Phase Noise Correction

Lasers used in the transmitter and the receiver local oscillator have a linewidth $\Delta\nu$ over which random frequency deviations occur, resulting in a phase noise in the signal. When discretized, the phase noise $\phi[k]$ can be modelled as a one-dimensional Gaussian random walk,

$$\phi[k] = \phi[k-1] + \Delta\phi_k$$
$$\text{where} \quad \Delta\phi_k \overset{\text{i.i.d.}}{\sim} \mathcal{N}(0, 2\pi\Delta\nu T_s) \quad \text{for all } k,$$

with T_s being the sampling period [4, §11.3].

The effect of phase noise can be most easily understood from a plot of the constellation, as shown in Figure 6a. Demodulation is impossible without any correction. Fortunately there are various techniques to mitigate this issue, and two of them are discussed below.

2.3.1 Differential PSK

In a normal PSK scheme, information is modulated as the phase of each transmitted symbol. In contrast, in differential PSK (DPSK), information is modulated as the *difference* in phase between two consecutive symbols [6, §7.3.2]. It can mitigate the effect of phase noise if the linewidth is small (such that $\Delta\phi_k$ is sufficiently smaller than, for example, $\pi/4$ for QPSK). Phase noise would then have little influence to the phase difference between consecutive symbols.

It was however noted that in DPSK, the demodulator is affected "twice" by phase noise. This increases the noise variance, making bit errors more likely [6, §7.3.2]. This can be seen (among other results) in Figure 8. This translates to a SNR penalty compared to the normal PSK scheme. At a BER of 10^{-3}, the penalty is about 2.5 dB.

2.3.2 Block phase noise estimation

The phase noise can also be estimated assuming the total phase noise over a small number of symbols is small. The Viterbi-Viterbi algorithm used is best illustrated by an example. Consider a QPSK scheme. At the receiver, the received signal $r[k]$ is given by

$$r[k] = \exp\left(\mathrm{j}\phi[k] + \mathrm{j}\frac{\pi}{4} + \mathrm{j}\frac{d[k]\pi}{2}\right) + n[k]$$

where $\phi[k]$ is the unknown phase of the kth symbol, $d[k] \in \{0, 1, 2, 3\}$ is the transmitted data, and $n[k]$ is AWGN. Taking the signal to the 4th power eliminates $d[k]$ from the expression, resulting in

$$r[k]^4 = \exp\left(\mathrm{j}4\phi[k] + \mathrm{j}\pi\right) + n'[k] \qquad (2)$$

where $n'[k]$ are the terms involving $n[k]$. It can be shown that $n'[k]$ has zero mean, thus if $\phi[k]$ does not vary much over a small range of k, then its value can be estimated by averaging over that range (thus eliminating $n'[k]$) [4, §11.5]. Figure 6b shows the algorithm estimating the phase of a noisy signal.

With a phase estimation method available, the effect of phase noise can be undone simply by adding a reversed phase shift.

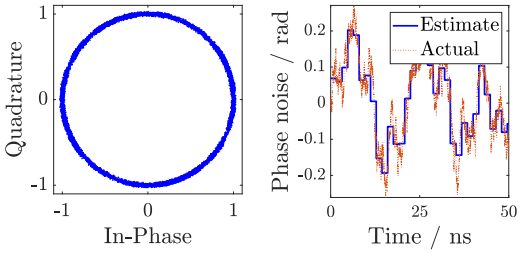

(a) Phase noise randomly rotating the constellation.

(b) Example of the Viterbi-Viterbi algorithm estimating phase noise.

Figure 6: Phase noise, and how it affects the received symbols.

However, at larger linewidths, phase estimation may make mistakes. This is due to the ambiguity in Equation (2), where in QPSK an additional phase increase of $\pi/2$ gives the same solution, and phase noise makes unambiguous phase unwrapping impossible. This is known as a *cycle slip* [7], and is illustrated in Figure 7.

The result of a particular run of the simulation is shown in Figure 8. It can be seen that when cycle slips do not occur, the resulting BER is much closer to the theoretical AWGN channel compared to DPSK. However, if a cycle slip occurs, all the subsequent symbols will be demodulated incorrectly [7], giving very poor performance.

To eliminate the effect of cycle slips, principles from DPSK can be incorporated into the phase estimation method, but instead of differentially modulating the *symbols*, the source *bit stream* is differentially *encoded*. This is known as *differentially encoded* PSK (DEPSK). At the receiver, the symbols are corrected after phase estimation (as above), and then demodulated like conventional PSK, before differentially decoding the bits. While this method transforms a single bit error into a pair of bit errors [7], it has a smaller SNR penalty than DPSK [8, Ch. 13], since the noise variance is not increased like it is in DPSK. Figure 8 also shows the result of DEPSK, which is immune to cycle slips, with a smaller SNR penalty than DPSK. Many forward error correction codes can effectively correct for short bursts of bit errors, thus further reducing the penalty [7], however this will not be investigated in this project.

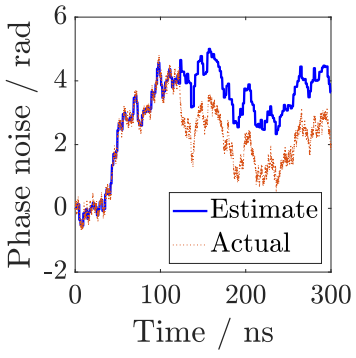

Figure 7: A cycle slip.

2.4 Non-linearity: Kerr Effect

Kerr effect is one of the non-linear effects investigated in this project. Kerr effect describes the change in refractive index

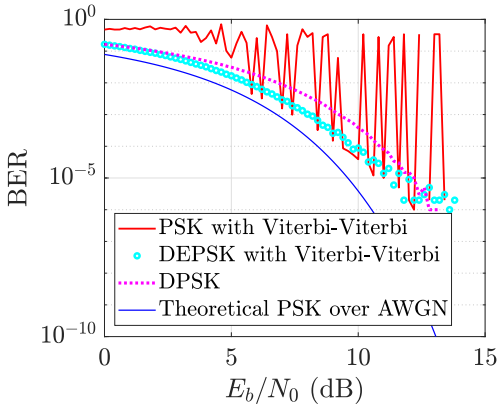

Figure 8: Performance of various methods under a phase noise of 10 MHz, on a particular run of the simulation.

of a material as the optical power of the incident beam changes. The result is a phase shift proportional to the optical power (i.e. the square of the electric field, hence non-linear) [4, §10.2], [9, §6.2.2]. To numerically simulate this effect together with other linear effects, the *split-step Fourier method* is used. In brief, the fibre length is divided into many small bits. The signal is first transformed to the Fourier domain, and chromatic dispersion is applied (as in Section 2.1). The signal is then transformed back to the time domain and its power is calculated. From this, the corresponding phase shift due to Kerr effect can be applied. This process repeats until the total simulated length reaches the desired transmission distance [9, §2.4.1, App. B].

Currently, the general structure of the split-step Fourier method has been coded, but there are small problems that require fixing, and as such results are yet to be included in this report. However, the general shape of the resulting curve matches existing literature [10], so there should be little difficulty in having it completed soon.

3 Future Plan and Timeline

After completing the simulation for Kerr effect, the most important task would be to integrate all the effects into a single simula-

tion program, to prepare for the final model to evaluate different transmission schemes. Afterwards, it was planned to have a more realistic model of the noise – the AWGN channel would be replaced with a combination of thermal noise (which can be modelled as AWGN) [11, §8.1.1] and shot noise. Finally, PDM and wavelength-division multiplexing would be implemented to have a "complete" model. To have sufficient time for the remaining parts of the project, it was planned to have this completed by week 3 of Lent term, i.e. about one week for each of the three tasks.

A few different designs of the network will be evaluated and compared, and the suitability to use in a PON will be discussed. Running the simulation a few times with different parameters should not take too much time, but discussing real-life feasibility may involve more review of current literature, so an estimate of 2 weeks is reserved for this.

The final three weeks of Lent will be spent obtaining experimental data and verifying simulation results, to make further adjustments to the model if necessary, and to prepare for the final report and presentation.

It is expected that most of the Easter vacation would be spent preparing for the examinations. Work on the final report and presentation would resume after that, which should be enough time to meet the deadline in week 5 of Easter term.

References

[1] C.C.K. Chan, "Protection architectures for passive optical networks," in *Passive Optical Networks: Principles and Practice*, C.F. Lam, Ed. Burlington, MA: Academic Press, 2007, pp. 243-266.

[2] J.S. Wey *et al.*, "Physical layer aspects of NG-PON2 standards – Part 1: optical link design," *J. Opt. Commun. Netw.*, vol. 8, no. 1, pp. 33-42, 2016. doi:10.1364/JOCN.8.000033

[3] D. Nesset, "PON Roadmap," *J. Opt. Commun. Netw.*, vol. 9, no. 1, pp. A71-A76, 2017. doi:10.1364/JOCN.9.000A71

[4] S. Kumar and M.J. Deen, *Fiber Optic Communications: Fundamentals and Applications*. Chichester, UK: Wiley, 2014.

[5] S.J. Savory, "Digital filters for coherent optical receivers," *Opt. Express*, vol. 16, no. 2, pp. 804-817, 2008. doi:10.1364/OE.16.000804

[6] J.G. Proakis and M. Salehi, *Contemporary Communication Systems Using MATLAB®*. Pacific Grove, CA: Brooks/Cole, 2000.

[7] M.G. Taylor, "Phase estimation methods for optical coherent detection using digital signal processing," *J. Lightwave Technol.*, vol. 27, no. 7, pp. 901-914, 2009. doi:10.1109/JLT.2008.927778

[8] The MathWorks, Inc., *Communications Toolbox™ User's Guide* (R2018b), 2018. [Online]. Available: <https://www.mathworks.com/help/pdf_doc/comm/comm.pdf>. [Accessed: Jan. 9, 2019].

[9] G.P. Agrawal, *Nonlinear Fiber Optics*, 5th ed. Oxford, UK: Academic Press, 2013.

[10] Md.S. Faruk, D.J. Ives, and S.J. Savory, "Technology requirements for an Alamouti-coded 100 Gb/s digital coherent receiver using 3×3 couplers for passive optical networks," *IEEE Photon. J.*, vol. 10, no. 1, 2018. doi:10.1109/JPHOT.2017.2788191

[11] P. Horowitz and W. Hill, *The Art of Electronics*, 3rd ed. New York: Cambridge University Press, 2015.